

## ION HEATING IN THE EXCITATION OF MAGNETO-ACOUSTIC OSCILLATIONS IN A PLASMA

I. A. KOVAN and A. M. SPEKTOR

Submitted May 19, 1967

Zh. Eksp. Teor. Fiz. 53, 1278–1286 (October, 1967)

Experiments on heating of magnetosonic waves in a uniform magnetic field are described. The gas-kinetic pressure  $nT$  measured on the basis of the diamagnetic effect is, under typical conditions ( $n_e \approx 10^{13}$ ,  $H_0 \approx 2$  kOe,  $T_e \approx 10$  eV), of the order of  $\sim 10^{15}$  eV/cm<sup>3</sup>. It is shown that the plasma pressure is due to protons whose mean thermal energy  $T_i \sim 100$  eV. The mechanism of ion heating is discussed.

## 1. INTRODUCTION

THE work reported here is a continuation of investigations undertaken to study magnetosonic resonance in a plasma. These experiments<sup>[1-3]</sup> were performed in systems with a homogeneous magnetic field. It was shown that excitation of magnetosonic oscillations in a plasma leads to heating of the electrons and the ions, and is also accompanied by generation of noise in a broad spectral interval. The electron temperature  $T_e$  in the discharge was measured, in the main, by double electric probes and ranged from 10 to 20 eV. The ion temperature  $T_i$  was not measured directly in these experiments. The lower limit of  $T_i$  was estimated from the Doppler width of the hydrogen lines and amounted to several electron volts. On the other hand, measurements were performed whose results pointed to an effective energy transfer from the high frequency generator to the plasma.

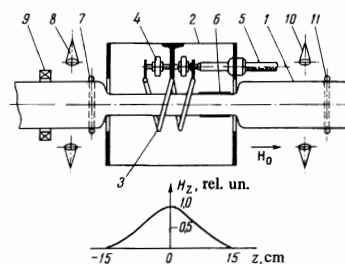
The present investigation was devoted, besides the questions connected with the specific features of the excitation of magnetosonic resonance, to a determination of the ion temperature, both by direct measurement and by estimating the energy balance between the observed energy and the energy carried away by the plasma to the side wall and to the ends of the apparatus.

## 2. DESCRIPTION OF EXPERIMENTAL SETUP

The experiments were made with a setup whose schematic diagram is shown in Fig. 1. The constant magnetic field of intensity up to 5 kOe was produced by a system of coils forming a solenoid  $\sim 2.5$  meters long. The cylindrical vacuum chamber of  $\sim 11$  cm diameter was made of glass and its diameter in the central section was reduced to 6 cm. Two auxiliary containers, of capacity  $\sim 100$  liters, were connected to the ends of the chamber and used to evacuate the gas. The initial pressure was  $p_0 \sim 2 \times 10^{-7}$  mm Hg.

The high-frequency generator circuit was made coaxial with the vacuum chamber in the central section of the latter. At a field intensity  $\tilde{H}_z \sim 75$  Oe, the generator, whose nominal power rating was 1.2 MW, could deliver  $\tilde{P} \sim 300$  kW to the load. The generator frequency was  $f = 21$  MHz. The variation of the frequency under the influence of the load (high-frequency discharge plasma) did not exceed 5 percent. The generator was matched to the plasma by means of a short-circuited loop. The investigations were made in the pulsed mode,

FIG. 1. Schematic diagram of apparatus: 1 – vacuum chamber, 2 – screen of high-frequency circuit, 3 – inductance of high-frequency circuit, 4 – capacitance of high-frequency circuit, 5 – high-frequency cable to the generator, 6 – short-circuited loop, 7 – loop for measurement of the field  $\tilde{H}_z$ , 8 – antennas of 8-mm interferometer, 9 – diamagnetic pickup, 10 – antennas of 4-mm interferometer, 11 – single-loop diamagnetic pickup.



using exponential pulses with a time constant  $\sim 15$  msec.

The arrangement of the measuring apparatus is shown in Fig. 1. The diamagnetic effect was observed in the plasma with the aid of two pickups located on both sides of the high-frequency circuit. The electron density  $n_e$  was measured simultaneously in the same sections, using two-beam interferometers operating at 4 and 8 mm. In addition, during the course of the experiments we registered the integral emission spectrum of the plasma in the visible region and the time variation of the intensity of the spectral lines. The power absorbed by the plasma was determined from the grid and cathode currents of the generator. The energy flux carried by the plasma to the ends of the apparatus was measured with a calorimeter. The alternating field  $\tilde{H}_z$  in the plasma was determined by means of a loop surrounding the chamber (Fig. 1).

## 3. DESCRIPTION OF EXPERIMENTS

The experiments were performed at a hydrogen working pressure  $p \sim 10^{-3}$  mm Hg and at the specified value of the magnetic field  $H_0$ . Several dozen microseconds after the high-frequency generator was turned on, breakdown was produced in the gas and led to formation of the plasma column. Contact between the plasma and the side walls of the chamber took place only in the region of the high-frequency circuit. The plasma flowed along the magnetic-field force lines and fell into the containers located at the ends, where it became neutralized. Owing to the large capacity of these containers, there was practically no reverse current of neutral gas, so that the duration of the process was determined by the time necessary to burn up the gas stored in the vol-

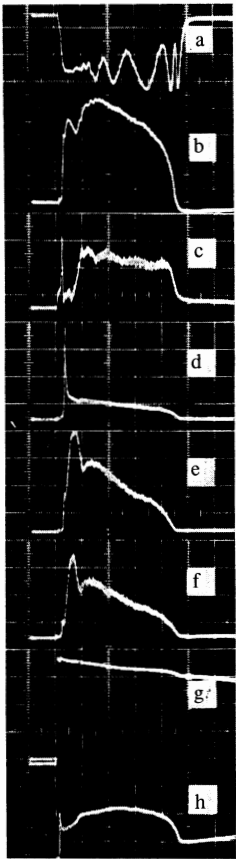


FIG. 2. Oscillograms of discharge in hydrogen. Field  $H_0 = 2$  kOe, sweep duration 0.5 msec/division.

ume and absorbed in the wall chambers.

The series of oscillograms shown in Fig. 2 gives an idea of the time variation of the main characteristics of the discharge in the hydrogen. Following the gas breakdown, the plasma density reaches a maximum value and then decreases smoothly (Fig. 2a). The rather large number of phase buildups on the interference pattern after the instant of cutoff makes it possible to conclude that the degree of inhomogeneity of the concentration, assuming a smooth radial distribution, does not exceed 10–15 percent. (It must be pointed out that the quantities  $n_e$  and  $nT$  were calculated for a 6 cm diameter, equal to the transverse dimension of the plasma column. Photography of the discharge in the monochromatic radiation of the individual lines has shown that the diameter of the glowing region is 5–6 cm., and that the distribution of the glow brightness over the radius is sufficiently uniform.)

The character of the variation of the diamagnetic signal (Fig. 2b) and of the amplitude of the wave field  $\tilde{H}_Z$  (Fig. 2c) indicates that these quantities are connected with the plasma density. The glow intensity of the neutral hydrogen (Fig. 2d) is characterized by a sharp maximum, the decrease of which is connected with the burning up of the gas in the volume. The subsequent weak glow is apparently maintained by the gas released from the surface of the chamber. The appearance in the discharge of oxygen and silicon impurities, the glow of which has a similar time behavior, is evidence that the material of the chamber wall ( $\text{SiO}_2$ ) evaporates. The variation of the intensity of the lines of the ions  $\text{O}^+$  and  $\text{Si}^{++}$  is illustrated by the oscillograms (Figs. 2e and 2f).

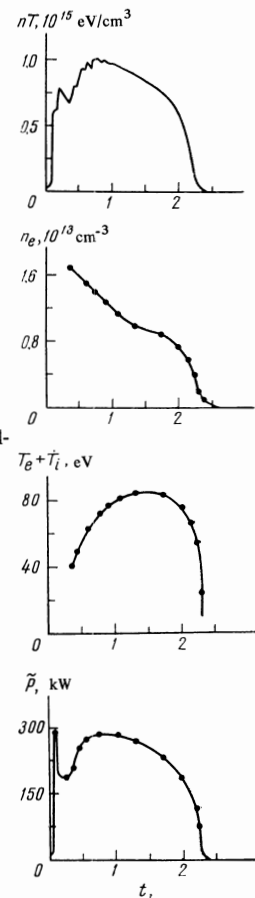


FIG. 3. Results of reduction of the oscillograms of Fig. 2 ( $t$  is in msec).

Finally, Figs. 2g and 2h show the oscillograms of the generator cathode and grid currents, from which the power delivered to the plasma was determined.

The results of the processing of the oscillograms are shown in Fig. 3. It follows from the obtained relations that in our experiment the transverse pressure  $nT$  reaches at the maximum a value  $10^{15}$  eV/cm<sup>3</sup>; the plasma concentration averaged over the time of the process is  $\bar{n}_e \sim 1.5 \times 10^{13}$  cm<sup>-3</sup>, the thermal energy of the charged particles ( $T_i + T_e$ ) exceeds 80 eV, and the power  $\bar{P}$  transferred to the plasma approaches 300 kW. The amplitude of the alternating field,  $\tilde{H}_Z \sim 50$ –60 Oe, was estimated under the assumption that the fundamental mode of the oscillations is excited in the plasma column. The good agreement between the absorbed power and the variation of the pressure in the plasma should be noted. It must be emphasized here that the magnitude of the diamagnetic signal is proportional to the square of the circuit voltage, i.e., proportional to the power delivered to the plasma by the generator.

The dependence of the transverse temperature ( $T_i + T_e$ ) on the concentration of the charged particles has a clearly pronounced maximum (Fig. 4). This plot was obtained from the  $n_e(t)$  and  $T_e + T_i = f(t)$  curves of Fig. 3. If we assume that such a variation is a manifestation of the magnetosonic resonance excited in the plasma column, then we can calculate the natural frequency of the oscillations. We use the expression for the oscillation frequency of an infinite cylinder with a free boundary<sup>[2,4]</sup>

$$f = 2.4H_0 / 2\pi r_0 \sqrt{4\pi\sigma}, \quad (1)$$

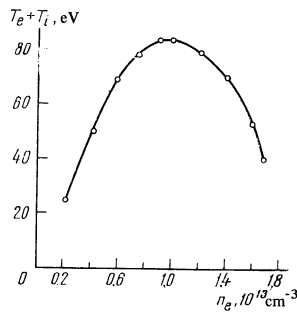


FIG. 4.

where  $H_0$  is the intensity of the magnetic field,  $r_0$  is the radius of the plasma cylinder,  $\rho$  is the density of the plasma per unit volume, and 2.4 is the first root of the Bessel function  $J_0(kr)$ . Substituting in (1) the value of the concentration corresponding to the maximum of the temperature, we get  $f = 18.6$  MHz, which agrees sufficiently well with the generator frequency  $f = 21$  MHz.

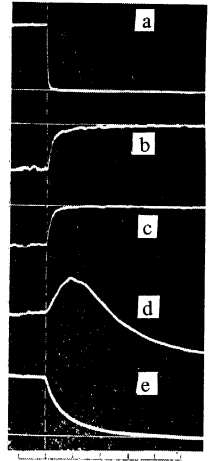
A study of the time-averaged plasma emission spectrum has made it possible to estimate the maximum electron temperature. In this experiment, the light of the discharge was focused with aid of a lens on the slit of a spectrograph (ISP-51) in a direction perpendicular to the force lines of the magnetic field. The exposure lasted 5–10 pulses. The spectrum revealed, besides the hydrogen lines, also the lines of oxygen  $O^I$ ,  $O^{II}$ , carbon  $C^{II}$ , nitrogen  $N^I$  and  $N^{II}$ , and silicon  $Si^{III}$ . There were no lines of higher degrees of ionization in the visible region, such as  $N^{III}$ . Inasmuch as the impurities enter into the discharge in the region of the high-frequency circuit, where the plasma may be in contact with the chamber walls, the absence of lines of doubly-charged nitrogen ions denotes the satisfaction of the following relation:

$$l/v_{\parallel} < 1/n_e \langle \sigma_i v_e \rangle. \quad (2)$$

Here  $l = 40$  cm—distance from the center of the high-frequency circuit to the center of the chamber from which the light is gathered,  $v_{\parallel} = \sqrt{k(T_e + T_i)/M} \approx 2 \times 10^6$  cm/sec is the maximum possible ion velocity along the force line of the field  $H_0$ ,  $\sigma_i(T_e)$  is the ionization cross section of the ion  $N^+$ , and  $v_e$  is the electron velocity. Substituting in (2) the value  $\bar{n}_e = 1.5 \times 10^{13}$  cm $^{-3}$ , corresponding to the electron density averaged over the pulse, we obtain, in accordance with the available data (see, e.g., [5]),  $T_e < 15$  eV.

Thus, the electron pressure  $nT_e \sim 2 \times 10^{14}$  eV/cm $^3$ , which can be ascribed to the plasma on the basis of the foregoing estimate, can not explain the observed diamagnetic effect. It is easy to show that the diamagnetic signal is likewise not determined by the pressure of the high-frequency field of the wave. Indeed,  $\tilde{H}_Z^2/8\pi \sim 10^{14}$  eV/cm $^3$  which is much lower than the measured value  $nT \sim 10^{15}$  eV/cm $^3$ .

For an independent confirmation of the foregoing conclusion, we performed the following experiment: within a time  $\sim 1$  msec after the start of the process, the high-frequency generator was switched off rapidly and the characteristics of the discharge in the afterglow were investigated. As follows from the oscillograms shown in Fig. 5, the amplitude of the high-frequency field  $\tilde{H}_Z$  (Fig. 5a) attenuates much more rapidly


 FIG. 5. Characteristics of discharge in afterglow. Sweep duration 20  $\mu$ sec/division.

than the remaining quantities. The time variation of the line intensities of the hydrogen (Fig. 5b) and of the singly-charged oxygen ion (Fig. 5c) is practically the same at the beginning of the decrease. When the line intensity decreases by a factor 3–4, these variations begin to diverge, and the brightness of the ion lines decreases more rapidly than the brightness of the neutral-atom lines. The decrease of the diamagnetic signal (Fig. 5d) and of the plasma density, which is determined from the readings of the 4-mm interferometer (Fig. 5d) is even slower than the variation of the line brightness. The foregoing relations are plotted in a semilog scale in Fig. 6.

The rapid decrease of the light intensity can be naturally explained as being due to the decrease in the electron temperature of the plasma, since the density of the charged particles remains practically constant during that time. The assumption that the density of the neutral hydrogen has time to change noticeably during the time of variation of the emission intensity is not very probable. As is well known, the intensity of the spectral line is determined by the expression

$$I = h\nu n_e n^* \int_{v_{min}}^{\infty} \sigma(v_e) v_e f(v_e) dv_e.$$

Here  $h\nu$  is the quantum energy,  $n^*$  is the number of emitters (atoms or ions) per unit volume,  $\sigma(v_e)$  is the excitation function of the line, and  $f(v_e)$  is the electron distribution function. Since the product in front of the integral is a constant independent of time, the rapid variation of the intensity is determined in this case only by the electron temperature.

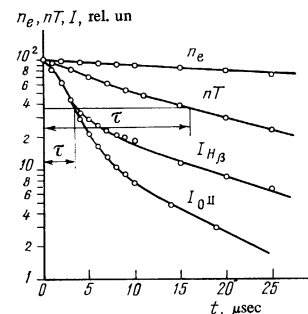


FIG. 6.

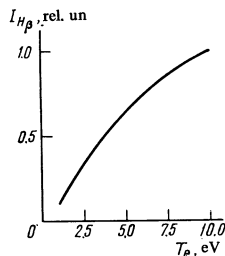


FIG. 7.

Figure 7 shows the dependence of the intensity  $I_{H\beta}$  on the temperature  $T_e$ , obtained by numerically integrating the experimental excitation cross section of the  $H\beta$  line over the Maxwellian velocity distribution. It follows from the plot that  $I_{H\beta}$  varies more slowly than  $T_e$ .

Thus, from a comparison of the rate of decrease of the alternating field  $\tilde{H}_z$  ( $\tau \lesssim 0.6 \mu\text{sec}$ ), the electron temperature  $T_e$  ( $\tau < 3 \mu\text{sec}$ ), and the pressure  $nT$  ( $\tau \sim 15 \mu\text{sec}$ ) we can state that the observed diamagnetic effect is determined completely by the plasma ion pressure.

To confirm the ion heating, we also measured the Doppler broadening of the spectral lines. The use of an ISP-51 spectrograph with a UF-85 camera ensured a linear dispersion 2–3 Å/mm in the investigated spectral interval. The radiation from the discharge was aimed on the slit of the instrument perpendicular to  $H_0$ . The exposure lasted 200 pulses. Figure 8 shows a comparison of a Gaussian contour (solid line) and the experimental contour (points) plotted for the  $O^{II}$  line ( $\lambda = 4414.9 \text{ \AA}$ ). The slight asymmetry of the experimental profile is connected with the temperature drift of the instrument. The measured half-width of the line ( $\delta\lambda \sim 0.4 \text{ \AA}$ ) greatly exceeded the apparatus half-width ( $\delta\lambda \sim 0.1 \text{ \AA}$ ). The broadening due to the Stark effect was negligibly small (the average density was  $\bar{n}_e \sim 1.5 \times 10^{13} \text{ cm}^{-3}$ ). The Zeeman splitting in a field  $H_0 = 2 \text{ kOe}$  was several hundredths of an Angstrom. Consequently, the main contribution to the observed broadening was made by the Doppler effect.

We processed in similar fashion the lines  $O^{II}$  ( $\lambda = 4351.3 \text{ \AA}$ ,  $\delta\lambda = 0.385 \text{ \AA}$ ),  $S_i^{III}$  ( $\lambda = 4552.5 \text{ \AA}$ ,  $\delta\lambda = 0.36 \text{ \AA}$ ), and  $H_\gamma$  ( $\lambda = 4340.5 \text{ \AA}$ ,  $\delta\lambda = 0.2 \text{ \AA}$ ). The temperature calculated from the half-width had the following values: for the oxygen ion  $\sim 20 \text{ eV}$ , for the doubly ionized silicon  $\sim 30 \text{ eV}$ , and for neutral hydrogen  $< 0.5 \text{ eV}$ .

It must be noted that the Larmor radius of the ions  $\rho_i$ , calculated on the basis of an estimate of  $T_i$  from the diamagnetic effect and also as a result of optical measurements, amounts to  $\sim 1 \text{ cm}$ , that is,  $\sim 30$  percent of the radius of the plasma column. Consequently, the value of  $nT$  may be underestimated by an approximate factor of 2. Therefore, even in this experiment the proton energy can exceed 100 eV.

Measurements of the energy flux escaping through the ends of the apparatus made it possible to draw certain conclusions concerning the mechanism of energy loss from the plasma. To this end, a calorimeter was placed at a distance  $\sim 60 \text{ cm}$  from the central plane of the high-frequency circuit on the axis of the chamber, and the energy given up in one discharge pulse was measured.

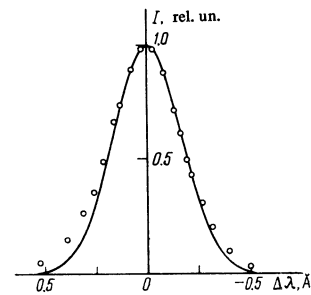


FIG. 8. Comparison of Gaussian (continuous curve) and experimental contour (points) of the  $O^{II}$  line;  $\lambda = 4414.9 \text{ \AA}$ ,  $\delta\lambda \sim 0.4 \text{ \AA}$ .

The power  $\tilde{P}$  calculated on the basis of this measurement and carried by the plasma along the force lines of the magnetic field  $H_0$  to the pickup was  $\sim 15 \text{ kW}$ . Simultaneously, we monitored near the calorimeter the density  $\bar{n}_e = 1.5 \times 10^{13} \text{ cm}^{-3}$  and the pressure  $\bar{n}T = 4 \times 10^{14} \text{ eV/cm}^3$ , averaged over the time of the process, and consequently we could estimate this power independently:

$$\tilde{P} = \frac{3}{2} n k T \sqrt{k T_i / M \pi r_0^2} = 14 \text{ kW}.$$

The good agreement between the presented values of  $\tilde{P}$  gives grounds for concluding that the energy transport along the magnetic field occurs at the thermal ion velocity.

The rapid decrease in the power registered by the calorimeter with increasing distance from the high-frequency circuit has shown that the plasma cools before it reaches the ends of the setup. This means that the energy loss occurs primarily transversely to the plasma column. Since the plasma was contained by the magnetic field and had no contact with the chamber walls, we must therefore exclude from consideration losses due to transverse diffusion, and regard the charge-exchange mechanism to be the most likely one.

Such an assumption was confirmed by the following results. Figure 9 shows the distribution of the pressure  $nT$  along the plasma column, plotted with the aid of two pickups, one of which could be moved in the direction of the  $z$  axis. It follows from these measurements that the pressure decreases by a factor  $e$  over a length  $l_0 \sim 70 \text{ cm}$ . If we attribute the decrease of  $nT$  to charge exchange, then we can determine the density of the neutral gas:

$$n_0 = 1 / \lambda \sigma \sim 2 \cdot 10^{12} \text{ cm}^{-3}$$

Here  $\lambda = \sqrt{3} l_0$  is the mean free path prior to the charge exchange for the ion in the magnetic field when the velocity distribution is isotropic and  $\sigma$  is the charge exchange cross section.

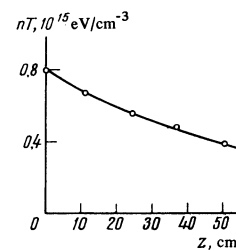


FIG. 9

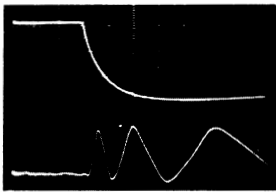


FIG. 10. Diamagnetic signal (upper curve) and interference pattern (lower curve). Sweep duration 10  $\mu\text{sec}/\text{division}$ .

Figure 10 shows the variation of the diamagnetic signal and of the phase variation of the 8-mm interferometer in the plasma afterglow regime. The pressure  $nT$  decreases exponentially with a time constant  $\tau \approx 8 \mu\text{sec}$ . Assuming that the decrease is due to charge exchange, let us calculate the density:

$$n_0 = 1/\tau \langle \sigma v_i \rangle = 2.5 \cdot 10^{12} \text{ cm}^{-3},$$

where  $v_i$  is the thermal velocity of the ions.

Thus, the neutral-gas density determined in two independent experiments coincides within the limits of experimental error. It should be noted that the relative ionization  $n_e/(n_e + n_0)$  is  $\sim 80$  percent, which agrees with the measurements of Kozlov and Rusanov<sup>[6]</sup>.

## DISCUSSION OF RESULTS

Our principal result is that the plasma ions are heated to energies  $\sim 10^2$  eV, whereas the temperature of the electrons in the discharge, unlike the data of Nazarov et al.<sup>[7]</sup>, remains sufficiently low,  $\sim 10$  eV. The relation  $T_i \approx T_e$ , which holds in the experiment, excludes the possibility of ion heating by Coulomb collisions with electrons. It is likewise improbable that the energy of the electromagnetic field of the wave is directly transferred to the ions as a result of their acceleration by harmonics of the cyclotron frequency  $\omega_i$ . Indeed, the frequency  $\omega$  of the forced oscillations of the plasma column is much higher than  $\omega_i$ , and the field energy should be absorbed by the protons at a harmonic  $n > 7$ . For the impurity ions, effective heating of which is also observed, the possible number of the harmonic is  $n > 100$ .

At the present stage of the research, no direct measurements were made of the longitudinal and radial distribution of the alternating field  $\vec{H}_z$ , but it can be assumed that for typical experimental conditions ( $H_0 \sim 2$  kOe,  $n_e \sim 10^{13} \text{ cm}^{-3}$ ), the excitation of radial magnetosonic oscillations is more likely to occur in the plasma (the plasma waveguide is beyond cutoff for longitudinal oscillations). In this case the energy of the wave is concentrated for the most part in the radial motion of the ions:

$$\frac{Mv_r^2}{2} \approx \frac{\vec{H}_z^2}{8\pi} \frac{1}{n_e},$$

and effective heating can occur as a result of the scattering of the translational motion by collisions, wherein the plasma temperature will increase during many periods of the oscillations. This is confirmed by the estimate of the time required to heat one particle:

$$t_h \sim \frac{3}{2} nkTV / \bar{P} \sim 1 \mu\text{sec};$$

here  $V$  is the volume of the plasma bounded by the high-frequency circuit, i.e.,  $t_h \sim 20$  T, where  $T$  is the period of the alternating-field oscillations.

It is easy to show that normal collisions make no noticeable contribution to the oscillation dissipation process. Indeed, the rather large value  $T_i \sim 10^2$  eV indicates that the ion energy cannot be increased by ion-ion collisions (the collision time is larger by three orders of magnitude than the period of the oscillations). Elastic collisions between ions and neutral atoms, which are characterized by sufficiently large cross section  $\sim 10^{-14} \text{ cm}^2$ , give only small-angle scattering and are likewise ineffective. Notice should be taken of the possibility of formation of out-of-phase ions (relative to the oscillations) as a result of the charge-exchange collisions or the ionization acts. These processes, however, cannot lead to the appearance of particles with an energy larger than the energy of the radial-mass motion

$$\frac{1}{2} Mv_r^2 \approx 10 \text{ eV} \ll kT_i.$$

Thus, to explain the observed effect of ion heating we must assume that there exist more effective collisions, as is possible, for example, when a turbulent state is produced in the plasma.

The authors are sincerely grateful to F. Zhachek for taking part in the optical measurements, and also B. I. Patrushev, I. M. Podgornyĭ, L. I. Rudakov, V. D. Rusanov, V. P. Smirnov, and D. A. Frank-Kamenetskiĭ for many numerous discussions. The authors are grateful to E. K. Zavoĭskiĭ for continuous interest in the work.

<sup>1</sup>D. A. Frank-Kamenetskiĭ, Zh. Tekh. Fiz. 30, 899 (1960) [Soviet Phys.-Tech. Phys. 5, 847 (1961)].

<sup>2</sup>I. A. Kovan, B. I. Patrushev, V. D. Rusanov, T. N. Tilinin, and D. A. Frank-Kamenetskiĭ, Zh. Eksp. Teor. Fiz. 43, 16 (1962) [Soviet Phys.-JETP 16, 10 (1963)].

<sup>3</sup>A. V. Borodin, I. A. Kovan, Ya. R. Rakhimbabaev, V. D. Rusanov, V. P. Smirnov, and D. A. Frank-Kamenetskiĭ, Nuclear Fusion 3, 38 (1963).

<sup>4</sup>A. V. Borodin, P. P. Gavrin, I. A. Kovan, B. I. Patrushev, S. L. Nedoseev, V. D. Rusanov, and D. A. Frank-Kamenetskiĭ, Zh. Eksp. Teor. Fiz. 41, 317 (1961) [Soviet Phys.-JETP 14, 228 (1962)].

<sup>5</sup>A. P. Vasil'ev, G. G. Dolgov-Savel'ev, and V. I. Kogan, Nuclear Fusion, 2, 655 (1962).

<sup>6</sup>O. V. Kozlov and V. D. Rusanov, *ibid.* 4, 312 (1964).

<sup>7</sup>N. I. Nazarov, A. I. Ermakov, V. V. Dolgopopolov, K. N. Stepanov, and V. T. Tolok, *ibid.* 3, 255 (1963).